Photogrammetrische Woche 1983
Institut für Photogrammetrie
Schriftenreihe, Heft 9, 1984

PHOTOGRAMMETRIC TARGET LOCATION TO SUBPIXEL ACCURACY IN DIGITAL IMAGES

E. Mikhail, West Lafayette

1. Introduction

The photogrammetrist is expected to increasingly deal with digital images. Such images are either directly acquired, as for example by push broom line arrays or multispectral scanners, or indirectly through digitizing photographs. The primary interest has been, and will continue to be, in the extraction of accurate geometric information from the images. This information often concerns well defined features such as edges, lines, crosses, and the like. Recent work at Purdue University |6| |7|, involved the measurement of digital images written on film with pixel sizes of 25, 50, and 100 μm. The primary objective was to determine how well a human operator can measure such images. Using synthetic images over real terrain data base, image measurement precisions of 7 μm for monoscopic, and 10 μm for stereoscopic, viewing were achieved even with pixel sizes up to 50 μm |7|. Using statistical design of experiment to analyze data from three observers measuring synthesized edges, it was found that each observer had a bias. Consequently, it was difficult to generalize the results of the experiment leading to the conclusion that significant variation exists between observers. In view of this, effort was concentrated on seeking methods for automatically locating targets in digital images and evaluating the accuracies.

Until recently, the method devised by Hueckel |1| was the only means of obtaining edge and line location estimates to subpixel levels, without applying interpolation. The work at the School of Electrical Engineering, Purdue University, devised another method where the first three moments calculated from the image are equated to their counterpart, calculated using a corresponding ideal edge |3|. At the School of Civil Engineering, Purdue University, we concentrated on a method which is based on least squares fit of ideal target to measured data. Preliminary results and comparisons have already been presented |4| |5|.

This paper will be devoted to methods and results for automatically locating geometric features in digital images. A quick review is given of such elementary features as: one-dimensional edge, one-dimensional pulse, two-dimensional edge, and two-dimensional line. More details are included for the common photogrammetric target of a cross. Emphasis is placed on data and numerical results instead of on mathematical derivations, the details of which are given in our technical reports.

2. Least squares location model

Let $f(s,t)$ represent the output of a perfect imaging system, that is, the ideal picture function. Consider next a linear, spatially-invariant imaging system with a normalized point-spread function $p(s,t)$ assumed known. Then let $\tilde{\ell}(s,t)$ denote a random variable representing the measurement at sampling position (s,t). We may model the measured quantity using the convolution

$$\tilde{\ell}(s,t) = \int_{-\infty}^{\infty}\int f(\xi,\eta)\, p(s-\xi,t-\eta)\, d\xi d\eta \qquad (1)$$

Consider now a set of u parameters $\underline{x}$ which completely characterizes $f(s,t)$ over the region of interest. Equation (1) may be rewritten as

$$\tilde{\ell}(s,t) - f(s,t;\underline{x}) * p(s,t) = 0 \qquad (2)$$

where * denotes the convolution operation.

Then for the ij-th picture element which is a sample of $\tilde{\ell}(s,t)$ at $s=s_i$, $t=t_j$, we may write a linearized condition equation of the form (dropping s,t for simplicity)

Photogrammetrische Woche 1983
Institut für Photogrammetrie
Schriftenreihe, Heft 9, 1984

$$\tilde{\ell}_{ij}^{0} + v_{ij} + \underline{B}_{ij}\underline{\Delta} = - F_{ij}(\underline{x}^{0}) \qquad (3)$$

where $\tilde{\ell}_{ij}^{0}$ is the initial estimate for the observation,

v_{ij} is the measurement residual,

$F_{ij}(\underline{x}) = - f_{ij}(\underline{x}) * P_{ij}$,

B_{ij} is the set of partial derivatives of $F_{ij}(\underline{x})$ with respect to the parameters, evaluated at $\underline{x} = \underline{x}^{0}$,

$\underline{x}^{0}$ is the set of initial parameter approximations, and

$\underline{\Delta}$ is the set of corrections to the parameter approximations.

Equation (3) represents a single condition equation for the model known as Adjustment by Indirect Observations. The total set of equations can then be solved by forming the normal equations in the conventional manner (2).

2.1 One-Dimensional Edge

Consider the ideal model of an edge or discontinuity present in a one-dimensional signal f(s), as shown in Figure 1. This may be expressed as

$$f(s) = h_1 + (h_2 - h_1)\, U(s - X) \qquad (4)$$

where U is the unit step function, or

$$U(s) = 1 \text{ for } s \geq 0 , \quad 0 \text{ for } s < 0$$

The one-dimensional form of equation (1) is:

$$\tilde{\ell}(s) = f(s) * p(s) \qquad (5)$$

where p(s) is the system line-spread function. It can be written in the linearized form of equation (3). If p(s) is a Gaussian function, the spread edge will take the general form depicted in Figure 2.

Other spread functions, as for example a rectangular function, can be used. It is also possible in the least squares solution to "self-calibrate" by estimating the parameters of the selected spread function. Thus, in addition to h_1, h_2, X (see Figure 1), a parameter, d, representing the width of the spread function is also estimated. Table 1 summarizes some of our early results.

On the basis of the results in Table 1 the following conclusions may be made: It should be noted, however, that the tests made were limited to simulated data with two types of spread-functions, and therefore all statements regarding the performance of the algorithms should be interpreted with this in mind.

1) The least squares model using a rectangular spread-function of known width did not function well in the presence of noise. This was due to the fact that there was no redundancy for the determination in the edge location, and because the form of the condition equations could lead to improper convergence when poor approximations were used.

2) The least squares model using a Gaussian spread-function of known width, performed well in the presence of noise. There was no instability associated with high levels of noise nor with the use of parameter approximations which were poorly selected.

3) The extended least squares model, in which the width of the edge spread was determined, performed well for both types of spread-function. It is believed that the case with the rectangular spread-function did not exhibit the same instability as previously because the number of measurements provided a redundancy for the determination of all parameters. This indicates that the original model would have operated satisfactorily if there had been more than one measurement in the spread area of the step.

Photogrammetrische Woche 1983
Institut für Photogrammetrie
Schriftenreihe, Heft 9, 1984

4) The precision of the estimate of edge location is dependent only upon the width of the spread-function and the signal-to-noise ratio. It does not appear to be adversely affected when the width of the spread-function must also be determined. The adjustment is also relatively insensitive to variations in the position of the edge within the area being modelled, provided that the edge is at a distance greater than the spread-width d from one extreme of the scanline.

5) Comparison with the method of edge location by moment preservation indicates that for the regular model the least squares fitting provides the better solution. For the extended model, the two methods give comparable results at low levels of signal noise. The most noticeable difference is for the case of perfect data, that is, without added noise, when the least squares method yields errors only due to round-off. In not case does the method using moment preservation yield smaller errors than by the least squares technique.

6) The extended least squares model has the advantages of providing estimates for both edge location and edge spread. However, when compared with the moment-preserving method it is computationally less efficient, and also requires initial approximations for all unknowns. The moment-preserving method contains a bias when the edge is not located near the center of the area under consideration. This is not believed to be a serious problem in most practical cases. The results indicate that the method of moment preservation offers a reliable solution to the problem, without requiring any assumptions or modelling of the spread-function. On the other hand, the method of least squares has the potential of providing higher accuracies particularly when started with good approximations as shown later on in this paper.

2.2 One-Dimensional Pulse

The concept of one-dimensional edge can be extended to the case of one-dimensional "line" or better termed as pulse. As depicted in Figure 3, four basic parameters are required for determining a pulse: h_1, h_2, X, and W. Detailed derivations for the least squares model leading to the linearized form of equation (3) are given in Thurgood and Mikhail |6|.

2.3 Two-Dimensional Edge and Line

A two-dimensional edge which is parallel to the t-axis, as shown in Figure 4, is treated in exactly the same manner as a one-dimensional edge. On the other hand, in the general case, the edge may make an angle θ with the t-axis, as shown in Figure 5. Consequently, it would require four parameters, h_1, h_2, X, θ to uniquely determine it in a given image.

A general two-dimensional line is shown in Figure 6. It is clear that, in addition to the four parameters needed for locating an edge, a fifth parameter, W, designating the line width, is required. The details of the derivations, and the attendant assumptions, are given in reference |6|.

2.4 Cross Targets

One of the most common photogrammetric targets is the cross, which is used in fiducial marks, in reseaus, or as man-made ground targets prior to photography. Therefore, our ultimate goal had been to develop our modeling to culminate with the cross target, then perform extensive experimentation with this type target. Figure 6 dealt with a line which continued beyond the limits of the image segment. By contrast, Figure 7 shows the case of a line of finite length, L, which is the last step before a cross. For such a line, we need to determine the coordinates of its center point, X and Y, as well as its length, L, and width, W, and orientation, θ. The model developed for a line of finite length can be extended to a more complex feature such as the cross shown in Figure 8. Here, the target is considered to be formed by a set of four rectangular components, R_i, $i = 1, \ldots, 4$, each with dimensions W by 1/2 (L - W). The center of the cross, determined by X,Y, falls outside all the four rectangles. As in the case of other simpler features, the details of the least squares algorithm used to automatically locate crosses are given in reference |6|.

Photogrammetrische Woche 1983
Institut für Photogrammetrie
Schriftenreihe, Heft 9, 1984

3. Experimentation with edge data

The first image feature considered for experimentation is the edge. Among others, an important objective was to analyze the performance of the least squares algorithm in locating an edge to subpixel levels.

3.1 Data Generation

In order to allow the fullest control over the geometric and densitometric nature of the images to be measured, simulated data was generated which represented a set of fifteen digital image files. Each file consisted of a two-dimensional array of size 1024 by 1024 pixels, containing grey shade distribution modeling a main image area. The mathematical model specifying the picture function within each image area was selected so as to allow the effects of the following parameters defining the edge to be assessed: edge type, width, contrast, orientation, and additive noise. Table 2 lists the specifications used in the generation of the 15 image files.

3.2 Image Preprocessing

When digital image files are written on film, as for example for visual measurement, they are affected by the spread function of the film-writer and emulsion. Therefore, to give more realism to the simulated digital edge data, a convolution was performed with a suitable spread function which was derived experimentally from the data.

3.3 Results from the Least Squares Algorithm

The results are shown in Table 3. As can be interpreted from the results from frame 1, the modeled spread function appears to fit a Gaussian function of width 0.82 pixels or a rectangular function of width 1.28 pixels. Errors in edge location estimates are general less than 0.050 pixels for those frames containing models of a ramp edge with high contrast and no noise (frames 2, 3, 4, 5, 11, 12), and corresponding errors in orientation estimates of less than 0.50°. Larger errors were obtained in frames 6, 7, and 9, with edge location estimates biased towards the lighter side of the idealized location by 0.04 - 0.20 pixels. These errors were a result of fitting the non-symmetric exponential-type data to the modeled symmetric function. Large errors were also obtained in the noisy edges, and in this instance, the two spread models did not give similar results. Overall, then, the adjustment appeared to operate well with edges which were symmetric in nature. The smoothing of the original data by the estimated spread function did not seem to affect the performance of the algorithm, probably because this modeled spread was assumed symmetric in nature itself.

3.4 Comparison with two other Methods

The same sets of data as described in the previous sections were input to the moment preserving and Hueckel two-dimensional edge operators. Both of these algorithms are generally used to yield estimates of edge position to subpixel levels in a direct manner. However, to guard against the introduction of possible biases into these estimates when the edge is not near the center of the image window being processed (to which both methods are sensitive), both methods were applied in an iterative approach which ensured that the final estimate of edge location lay within one pixel's distance of the center of the 9 by 9 window used.

The results of using these two algorithms for the fifteen edge frames are shown in Table 4. As can be seen, the errors in the edge location estimates are less than 0.05 pixel for those high contrast images with symmetric edge data (frames 1-5, 8, 12, 13). The Hueckel operator tends to point towards the lighter side of the edge when compared with the moment preserving method, even in the case of the perfect step data. The average size of this difference between two methods is still only about 0.05 pixel. Larger errors are associated with frames 6, 7, and 9, which contain asymmetric edges, and with certain frames containing added

Photogrammetrische Woche 1983
Institut für Photogrammetrie
Schriftenreihe, Heft 9, 1984

noise. In fact, the effect of added noise is only distinct in frame 15 (40% noise) for the moment preserving algorithm, and in frame 14 (20% noise) for the Hueckel operation. For noiseless frames, the estimates of orientation are in error only for frame 11, which contained the rotated edge at 22 1/2 °, and then only to the order of 0.2 ° for the moment preserving and 0.8 ° for the Hueckel method. Errors of up to 13° were associated with the frames to which noise had been added.

Overall, the results are consistent with those obtained by the least squares algorithms. The moment preserving method in particular yielded edge locations to within 0.05 pixels of the least squares estimates for twelve out of the fifteen frames. However, this is a very small sample of results from which to draw many general conclusions.

4. Experimentation with Cross Data

The main task of this effort is composed of two steps: (1) The detection and approximate location of the cross target, and (2) Precise determination of the center of the target using the least squares algorithm. With regard to step (1), the optimum approach is to have an automated procedure, based upon pattern recognition and feature extraction techniques, which would scan an entire image and produce the locations of all crosses. At the early stages of this research, we limited consideration to one target within a large window. In order to calculate approximations for the target parameters, a simple method using templates and cross-correlation was used. A set of six templates, representing target orientations varying from -34° to 45°, is shown in Figure 9. Simple procedures were also used to derive approximations for cross and background shades. Thus, all five approximate values X^o, Y^o, θ^o, h_1^o, h_2^o were computed before entering into the rigorous least squares adjustment algorithm. In these early investigations, the length, L, and width, W, of the crosses are assumed known.

4.1 Fort Sill Synthetic Images

The digital image files generated for the purpose of measuring the positions of crosses made use of the simulation package SIM previously developed at Purdue University and fully described by Unruh et al [8]. SIM makes use of an augmented digital data base containing both elevation information and quantized density values from a digitized orthophotograph. This is the source from which imagery may be generated which bears the attributes of an aerial frame photograph, but in a digital form. The data base used contained 1778 rows by 1117 columns each, representing the Fort Sill area of Oklahoma. It was derived from aerial photography flown at a nominal scale of 1 : 50 000 , and the spacing between data base elements amounts to 4.8 meters at ground scale. The surface defined represents rolling terrain, with elevations ranging from 350 to 550 meters above sea level.

The program makes use of the colinearity condition as the basis for defining an artificial photo ray which systematically scans the object space. The appropriate image element grey shade is assigned by first determining the intersection of the photo ray and the object space surface, and then applying suitable interpolation in grey shade from the four adjacent data base elements. By searching for the surface intersection closest to the camera station, hidden surfaces are effectively removed. The images thus produced simulate the photographic perspective with user-defined interior and exterior orientations, with all inherent displacements due to relief and tilt. As presently written, SIM uses a bilinear interpolation in elevation and in grey shade, but both can be redefined easily.

It is possible to superimpose artificial targets in the terrain model by assigning new grey shade values to specific data base elements. In this way, such targets are included in the image synthesis process, and appear as other natural features in the resultant digital image file. By recording the location of the data base elements modified, the ideal location of the imaged target may be easily determined. This provides a set of ideal image coordinates, which are used to evaluate the errors associated with a given target positioning algorithm. Such an approach has been used in the past in the hardcopy measurement of dot and cross targets, by Unruh and Mikhail [7].

Photogrammetrische Woche 1983
Institut für Photogrammetrie
Schriftenreihe, Heft 9, 1984

Minor modification of the SIM package was made to permit the generation of several image segments within one program execution, each with the same interior and exterior orientations, but containing only a small portion of the whole image. A single image coordinate system was preserved by the recording of a false origin for each sub-image. Therefore, the location of any feature could be referenced to an overall image system defined by the orientation parameters. This approach was implemented to allow the efficient use of SIM, since it was not at all necessary to generate a large image, but only a set of small images each containing a feature of interest, all referenced to one coordinate system.

In one experiment, a set of nine image files were generated. The exterior orientation was varied, by assigning combinations of three different values of the primary rotation omega (ω) and three different values of the tertiary rotation kappa (κ). Thus kappa took on values 0°, 20°, and 45°, and omega 0°, 5°, and 15°. Within one file, eight cross targets were imaged. In all cases the ratio (average pixel spacing)/(data base element spacing) was very roughly 1.0. Therefore the approximate dimensions of the crosses in the resultant images were 5 pixel's length by 1 pixel's width.

Table 5 summarizes the results from the first set of experiments. As mentioned previously two types of spread functions were used, the rectangular and gaussian.

The range in root mean square errors in $\hat{X}$ or $\hat{Y}$ is from 0.033 to 0.086 pixel, with one case yielding the relatively high value of 0.394. It can be seen in Table 5 that the low accuracy levels associated with the imagery with kappa of 45° and omega of 5° are accompanied by large values of root mean square error in θ. Closer examination revealed that these values are larger than the average due to the poor performance of the pointing algorithms in two instances. In these particular instances, the initial approximations for θ were 0°, when in fact the true values should have been close to kappa (45°). These poor approximations appear to have allowed convergence of the adjustments to local minima, and the resultant residuals in the final estimates were on the order of 45° in orientation and 1.0 pixel in position.

4.2 Further Experiments With Fort Sill Image Data

The problem of proper approximations for the parameters was demonstrated in the preceding section, Table 5. Furthermore, the amount of effort required to deal with each target individually, made it clear that a more general procedure is needed. At the School of Electrical Engineering a moment-based method was devised that dealt with both requirements; it allowed the automatic recognition and location of several crosses in an image, and provided good approximations for the parameters to be used in the least squares algorithm for more precise position estimation. This section documents results of experiments designed for the purpose of evaluating this method.

A modification to the SIM program was made to enable 20 crosses per data base segment to be imposed on the Fort Sill data base. Four different cross sizes were used: 1 by 5, 1 by 7, 2 by 6, and 2 by 8 pixels. These sizes were intended to be more realistic than the 1 by 3 and 1 by 5 pixels used earlier.

Six image segments were synthesized at varying orientations and camera positions. The total image file containing multiple crosses of different sizes and orientation was used to test various possibilities of target detection and location.

Table 6 summarizes the results from this image file of six segments, listing the discrepancies, ΔX, ΔY, between ideal and estimated target coordinates. The first two columns give the values of ΔX, ΔY from the moment-based method. The RMS in 0.136 pixel in X and 0.093 pixel in Y. The following two columns contain the results from the least squares algorithm with rectangular spread function, using the very simple template matching method for calculating the parameter approximations. The last two columns of discrepancies correspond to the case of using the moment method to provide approximations for the least squares method. Table 7, gives the results obtained when the Gaussian spread function is used.

It is clear from both of these tables that the moment-based method followed by the least squares method provided the best results.

Photogrammetrische Woche 1983
Institut für Photogrammetrie
Schriftenreihe, Heft 9, 1984

4.3 Experiments With the Arizona Test Data

The Fort Sill image file generated as described in the preceding section provided an image which was somewhat "blocky". Therefore, another test image was obtained by generating cross targets on a digital image using the Arizona test data. This test data was derived from a digitized stereo model formed by two nearly vertical images taken in October 1966 near Guadelupe, Arizona. The cross targets were superimposed on the digitized image.

A 512 x 512 segment of the digital image is used. Twenty-five cross targets were randomly selected and placed on the image. Cross sizes with aspect ratios of 1 : 7, 1 : 10, and 1 : 13 were used. The crosses were arbitrarily rotated to various orientation angles. Furthermore, noise was added to the crosses according to a distribution having the same standard deviation as the image background around each cross. It is recognized that this is a rather severe amount of noise, but we felt that if the algorithms performed reasonably in this case that we can be confident of the results from other cases with less noise.

Table 8 lists the discrepancies at the 25 crosses for four different cases. Case A is the moment-based method. In case B, only the values of X, Y, Θ from the moment method are used as approximations in the least squares algorithm. In case C, all five values of X, Y, Θ, h_1, h_2 are entered into the least squares algorithm. Finally, case D is the same as case C, except that instead of using fixed values for the length, L, and width, W, of the cross, a simple routine is written to estimate these two parameters prior to entering into the least squares algorithm. The last case, D, gives the lowest RMS values, of about 0.05 pixel in X and 0.03 pixel in Y, and may therefore be considered as the best that we can expect.

5. Conclusions

1) The least squares algorithm is a powerful tool for automatically locating features of interest to the photogrammetrist, such as edges, lines, and crosses. However, since the condition equations are non-linear, approximations are necessary for the parameters.

2) Except with very few exceptions (where the approximations are quite poor) the least squares method was capable of locating an edge to a fraction of a pixel. It also compared favorably with two other methods, the moment-preserving and Hueckel.

3) Pattern recognition and feature extraction methods are capable of providing locations for the centers of the cross targets to less than 0.20 pixels in each of the X- and Y-directions.

4) The least squares algorithm, with approximations derived by very simple techniques, produces results to less than 0.1 pixel in each of the two axes.

5) Using the results from the pattern recognition and feature extraction algorithms as approximations into the least squares algorithm leads to cross target locations to 0.05 pixel or less in each axis. This is considered the optimum result possible with the data and methods employed.

6) With the pointing accuracy established to 0.05 or less in X and Y, subsequent effort will apply these techniques to the determination of the effect of digital image processing operations on the geometric integrity of the images.

Acknowledgements

The work described in this paper has been supported by the U.S. Army Research Office under Contract No. DAAG 29-81-K-0063. The author expresses his gratitude to Dr. Steven Mock, the Scientific Program Director. Thanks are also expressed to Dr. J.D. Thurgood of Wild Heerbrugg who worked on the project while a graduate student at Purdue University. The author would also like to thank Prof. O.R. Mitchell and Mr. Mark Akey of the School of Electrical Engineering at Purdue University for their valuable assistance, and to J.S. Bethel, D.B. Cantiller, and W.A. Oren of the School of Civil Engineering for assistance with various programming tasks.

Photogrammetrische Woche 1983
Institut für Photogrammetrie
Schriftenreihe, Heft 9, 1984

REFERENCES

|1| Hueckel, M.H., A Local Visual Operator which recognizes Edges and Lines", J. Association for Computing Machinery, Vol. 20, 1973.

|2| Mikhail, E.M., Unruh, J.E., and Alspaugh, D.H., Image Simulation from Digital Data, 1977, Proceedings of the Fall Technical Meeting of the American Society of Photogrammetry, 1977.

|3| Tabatabai, A.J. and Mitchell, O.R., Edge Location to Subpixel Accuracy in Digital Imagery, submitted to IEEE Trans. on Pattern Analysis and Machine Intelligence, 1981.

|4| Thurgood, J.D. and Mikhail, E.M., Photogrammetric Aspects of Digital Images, Proceedings of the 48th Annual Meeting of the American Society of Photogrammetry, pp. 295-304, 1982.

|5| Thurgood, J.D. and Mikhail, E.M., Photogrammetric Analysis of Digital Images, Proceedings of Commission III Symposium of the International Society for Photogrammetry and Remote Sensing, Helsinki, June 1982.

|6| Thurgood, J.D. and Mikhail, E.M., Subpixel Mensuration of Photogrammetric Targets in Digital Images, Technical Report, School of Civil Engineering, Purdue University, No. CH-PH-82-2, August 1982.

|7| Unruh, J.E. and Mikhail, E.M., Digital Image Simulation for Photogrammetric Applications, Technical Report, School of Civil Engineering, Purdue University, No. CE-PH-81-1, 1981.

|8| Unruh, J.E., Alspaugh, D.H., and Mikhail, E.M., Sensor Simulation from Spectral and Digital Terrain Data, Final Technical Report, for the Defense Mapping Agency Aerospace Center, St. Louis, under DMA Contract 700-75-c-0119, 1977.

Abstract

The location of well defined targets, such as edges, lines, and crosses, in digital images can be determined automatically using suitably designed algorithms. Unlike human measurements of such targets on hardcopy, where there are wide variations within and between observers, automated mensuration is perfectly repeatable. The primary question therefore concerns not the precision, but the accuracy of the results from these algorithms. Experimentation with synthetic digital images generated from a real terrain digital data base indicates that subpixel accuracies can be achieved.

The basic concept is to use a least squares adjustment model to match the ideal geometric shape of the target (edge, line, or cross) to its measured data. The adjustment yields estimates of the parameters that describe the geometric location of the target, as well as the grey levels within and around the target. The main task here is the precise location of a target, the shape of which is known a priori.

More recent work is attempting to first detect the presence of the targets and then locate them. The process in this case relies heavily on the two-dimensional moments of the targets. If the type of target is known (e.g. a cross), the algorithm will classify it as such. Comparisons are made between the results from this more general algorithm, and the least squares algorithm. Whenever feasible, the results from the former may be used as approximations into the latter to determine if further accuracy improvement may be attained.

Photogrammetrische Woche 1983
Institut für Photogrammetrie
Schriftenreihe, Heft 9, 1984

PHOTOGRAMMETRISCHE ZIELBESTIMMUNG MIT SUB-PIXEL-GENAUIGKEIT IN DIGITALEN BILDERN

Zusammenfassung

Mit geeigneten Algorithmen kann die Lage gut definierter Ziele wie Kanten, Linien und Kreuze in digitalen Bildern automatisch bestimmt werden. Im Gegensatz zur Bestimmung solcher Ziele auf Papier durch Menschen, bei der besonders beim Einsatz mehrerer Auswerter große Abweichungen auftreten, ergeben automatische Messungen immer die gleiche Eindeutigkeit. Das Hauptaugenmerk richtet sich also nicht auf die Genauigkeit, sondern auf die Richtigkeit der Ergebnisse dieser Algorithmen. Versuche mit synthetischen digitalen Bildern, die mit Hilfe einer echten Geländedatenbank erzeugt wurden, zeigen, daß Sub-Pixel-Präzision erreicht werden kann.

Das Grundprinzip beruht auf dem Einsatz eines Ausgleichungsverfahrens der kleinsten Quadrate zur Anpassung der idealen geometrischen Form des Ziels (Kante, Linie, Kreuz) an die gemessenen Daten. Die Ausgleichung ergibt Näherungswerte für die Parameter, die die geometrische Lage des Ziels beschreiben, sowie die Grauwerte im und um das Ziel herum. Die Hauptaufgabe ist also die präzise Lagebestimmung eines Ziels, dessen Form bekannt ist.

In neueren Arbeiten wird versucht, erst festzustellen, ob ein Ziel vorhanden ist, und dann dessen Lage zu bestimmen. Dabei stützt man sich sehr stark auf die zweidimensionalen Aspekte der Ziele. Wenn die Art des Ziels bekannt ist, z.B. ein Kreuz, dann wird es vom Algorithmus erkannt. Dann werden die Ergebnisse des ersten Algorithmus als Näherungswerte für den zweiten benutzt werden, wenn damit eine Genauigkeitsverbesserung erreicht werden kann.

MESURE DE POINTS PHOTOGRAMMETRIQUES SUR DES IMAGES NUMERIQUES AVEC UNE PRECISION SUPERIEURE AUX DIMENSIONS DE LA SURFACE D'OBSERVATION (SUB-PIXEL)

Résumé

La position planimétrique d'objets bien définis dans une image numérique, tels que des ruptures de pente, des lignes ou des croix, se laisse déterminer automatiquement avec des algorithmes appropriés. Contrairement à la mesure de tels objects sur le papier où intervient las subjectivité humaine et où de grandes différences peuvent apparaître quand plusieurs opérateurs se remplacent dans ce travail, ces mesures automatiques sont d'une parfaite répétablilité. Par conséquent, le problème primaire ne concerne pas la précision, mais l'exactitude des résultats fournis par les algorithmes. Les essais qui ont été faits avec des images numériques synthétisées sur la base de données de terrain réelles, ont montré qu'on peut atteindre la précision du sub-pixel.

Le principe se base sur un procédé de compensation selon la méthode des moindres carrés pour la corrélation entre la forme géométrique idéale de l'objet (rupture de pente, ligne où croix) et les données mesurées. La compensation fournit des valeurs approximatives pour les paramètres qui décrivent la position géométrique de l'objet ainsi que les niveaux de gris dans et autour de l'objet en question. Le but principal est donc la localisation précise d'un objet dont la forme est connue à priori.

De nouveaux travaux ont été entrepris dans le but de parvenir à détecter la présence d'un objet avant d'en déterminer sa position. Ce processus s'appuie largement sur les aspects bidimensionnels de l'objet. Lorsque la nature de celui-ci est connue, c'est une croix par exemple, l'algorithme est en mesure de classer l'objet comme tel. Les résultats de cet algorithme plus général sont ensuite comparés à ceux de l'algorithme des moindres carrés. Dans la mesure où ceci est faisable, les résultats du premier algorithme sont utilisés comme valeurs approximatives pour le second, si une amélioration de la précision peut être attendue.

Photogrammetrische Woche 1983
Institut für Photogrammetrie
Schriftenreihe, Heft 9, 1984

LA MEDICION DE PUNTOS FOTOGRAMETRICOS EN IMAGENES DIGITALES CON PRECISION SUPERIOR AL TAMANO DEL AREA DE EXPLORACION (PIXEL)

Resumen

Unos algoritmos adecuados permiten determinar automáticamente en imágenes digitales la situación de objetos bien definidos, tales como cantos del terreno, líneas y cruces. Contrariamente a la determinación en el fotograma de este tipo de objetos por personas, donde es muy amplia la gama de variación, sobre todo al intervenir varios operadores, las mediciones automáticas siempre proporcionan resultados inequívocos. Por lo tanto, lo que importa principalmente no es la precisión, sino más bien los resultados correctos de estos algoritmos. Las experiencias hechas con imágenes digitales sintéticas, generadas con ayuda de un auténtico banco de datos del terreno, ha demostrado que puede lograrse precisión superior al pixel.

El principio se basa en la aplicación de un método de compensación de mínimos cuadrados para adaptar la forma geométrica ideal del objeto (canto, línea, cruz) a los datos medidos. El resultado de la compensación son valores de aproximación para los parámetros que describen la situación geométrica del objeto así como valores de grises en el objeto y alrededor del mismo. El problema principal es la determinación precisa de la situación de un objeto de forma conocida.

En trabajos más recientes se trata de hacer constar en primer lugar si efectivamente hay un objeto y a continuación se procede a determinar su situación para lo cual se recurre ampliamente a los aspectos bidimensionales de los objetos. Cuando se conoce la índole del objeto, p. ej. una cruz, el algoritmo lo clasifica como tal y a continuación, los resultados de este algoritmo se comparan con los del algoritmo de mínimos cuadrados. Siempre que sea factible se utilizarán los resultados del primer algoritmo en calidad de valores de aproximación para el segundo, a condición de que ello permita incrementar la precisión.

Prof. Edward M. Mikhail
Purdue University,
School of Civil Engineering
West Lafayette, Indiana 47907, USA

Photogrammetrische Woche 1983
Institut für Photogrammetrie
Schriftenreihe, Heft 9, 1984

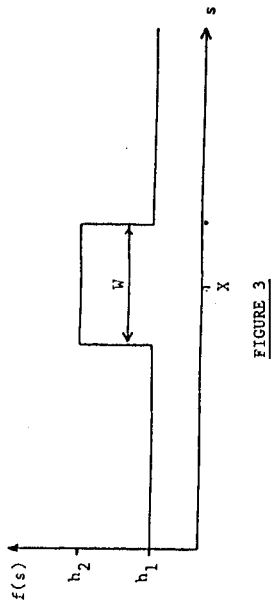

FIGURE 3

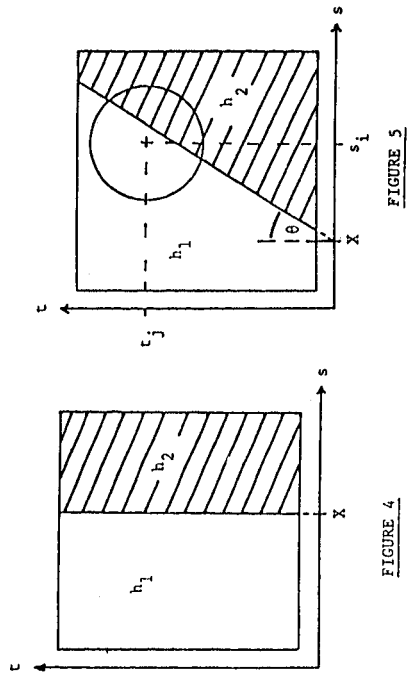

FIGURE 5

FIGURE 4

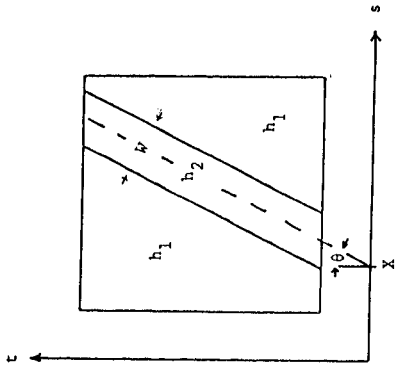

FIGURE 6

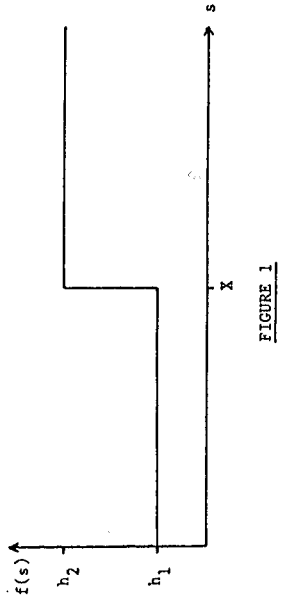

FIGURE 1

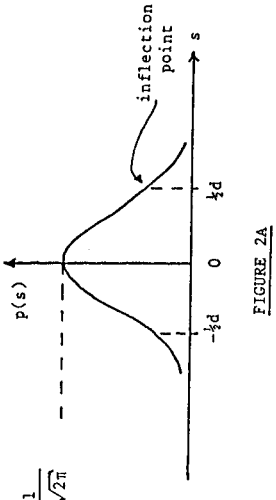

FIGURE 2A

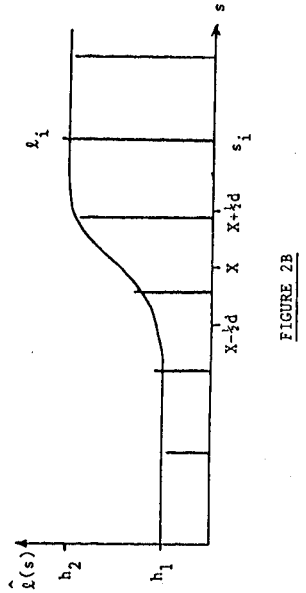

FIGURE 2B

Photogrammetrische Woche 1983
Institut für Photogrammetrie
Schriftenreihe, Heft 9, 1984

FIGURE 9

FIGURE 7

FIGURE 8

TABLE 1. EDGE POINTING WITH SIMULATED DATA

DATA CHARACTERISTICS			ROOT MEAN SQUARE ERROR (X) (in pixels)	
SPREAD WIDTH	SPREAD TYPE	NOISE LEVEL	MOMENT PRESERVING	LEAST SQUARES
1 pixel	RECTANG.	0	0.073	0.000
		1%	0.074	0.010*
		10%	0.192	0.106*
	GAUSSIAN	0	0.027	0.003
		1%	0.032	0.015
		10%	0.223	0.164
assumed unknown	RECTANG.	0	0.007	0.000
		1%	0.024	0.023
		10%	0.299	0.231
	GAUSSIAN	0	0.011	0.000
		1%	0.033	0.033
		10%	0.384	0.346

* only achieved using best parameter approximations.

TABLE 2. SPECIFICATIONS FOR IMAGE FILES CONTAINING EDGES

EDGE PROFILE	SPREAD WIDTH (pixels)	POSITION OF EDGE[1]	COMMENTS
1. step	-	X=490.5	perfect step edge
2. ramp	2	X=491.0	centered on pixel
3. ramp	2	X=490.76	off-centered
4. ramp	4	X=492.0	centered
5. ramp	4	X=491.76	off-centered
6. exponential	2	X=491.21	
7. exponential	4	X=492.41	
8. raised cosine	4	X=492.0	
9. exp (rsed cos)	4	X=492.41	
10. step	-	X=490.5	low contrast
11. ramp	2	X=703.49-Ytan22½°	oriented at 22½°
12. ramp	2	X=1004-Y	oriented at 45°
13. ramp	2	X=491.0	added noise σ_n=35
14. ramp	2	X=491.0	added noise σ_n=20
15. ramp	4	X=492.0	added noise σ_n=40

[1] Locus of points in ideal image surface with the mean value of grey shade: X=column number, Y=row number within the image array.

TABLE 3. RESULTS OF EDGE-POINTING USING LEAST SQUARES

FRAME	RECTANG. MODEL		$\hat{d}$	GAUSSIAN MODEL		$\hat{d}$
	$v(\hat{X})$	$v(\hat{\theta})$		$v(\hat{X})$	$v(\hat{\theta})$	
1	0.	0.	1.28	0.	0.	0.82
2	0.	0.	2.27	0.	0.	1.29
3	-.008	0.	2.20	.018	0.	1.53
4	.003	0.	4.21	-.022	0.	2.72
5	0.	0.	4.10	-.007	0.	2.82
6	-.041	0.	1.94	-.088	0.	1.22
7	-.119	0.05	3.80	-.112	0.	2.59
8	.003	0.	2.98	-.002	0.	2.09
9	-.207	0.05	3.06	-.176	0.	2.04
10	.099	0.	1.01	0.	0.	0.78
11	.037	0.55	1.80	.036	0.70	1.32
12	.001	0.	1.72	0.	0.01	1.05
13	-.191	-1.77	2.14	-.132	-2.61	1.02
14	-.034	-1.71	1.01	-.080	-1.61	1.16
15	-.451	6.63	2.46	-.081	3.15	3.05

$v(\hat{X})$ and $v(\hat{\theta})$ - true errors in X (pixels) and θ (degrees) respectively.

TABLE 4. RESULTS OF EDGE-POINTING USING THE MOMENT PRESERVING AND HUECKEL OPERATORS

FRAME	MOMENT PRESERVING		HUECKEL OPERATOR	
	$v(\hat{X})$	$v(\hat{\theta})$	$v(\hat{X})$	$v(\hat{\theta})$
1	-.003	0.	-.030	0.
2	0.	0.	-.041	0.
3	.029	0.	-.042	0.
4	0.	0.	-.045	0.
5	.047	0.	-.012	0.
6	-.077	0.	-.139	0.
7	-.104	0.	-.208	0.
8	0.	0.	-.043	0.
9	-.182	0.	-.244	0.
10	-.003	0.	-.079	0.
11	0.	0.18	-.041	0.78
12	0.	0.	-.042	0.
13	-.018	4.84	0.42[1]	3.49
14	-.038	2.64	.959	1.59
15	-.621	7.06	.084	13.42

$v(\hat{X})$ and $v(\hat{\theta})$ - true errors in $\hat{X}$ (pixels) and $\hat{\theta}$ (degrees) respectively.

TABLE 5. CROSS POINTING ON IMAGERY WITH VARIOUS ORIENTATIONS - TYPE 1 TARGET

IMAGE κ	IMAGE ω	WITH RECTANGULAR SPREAD MODEL RMSE ($\hat{X}$ or $\hat{Y}$) (pixels)	RMSE ($\hat{\theta}$) (degrees)	RM ($\hat{\sigma}_0^2$) (grey levels)	WITH GAUSSIAN SPREAD MODEL RMSE ($\hat{X}$ or $\hat{Y}$) (pixels)	RMSE ($\hat{\theta}$) (degrees)	RM ($\hat{\sigma}_0^2$) (grey levels)
0	0	.051	0.98	13.9	.086	1.55	13.7
	5°	.052	1.98	13.9	.041	1.53	13.5
	15°	.062	2.38	14.2	.054	2.70	13.6
20°	0	.065	1.38	14.0	.066	2.14	13.7
	5°	.041	1.66	13.5	.048	2.36	13.1
	15°	.045	2.80	13.0	.048	3.01	12.7
45°	0	.033	0.98	12.7	.040	1.20	12.6
	5°	.394	22.14	16.7	.390	22.02	16.6
	15°	.041	2.68	13.1	.038	2.63	12.6

Each image contains eight type 1 cross targets of dimensions roughly 5 by 1 pixels.

TABLE 6.

IMAGE TARGET	MOMENT ΔX	MOMENT ΔY	RECTANGULAR SPREAD FUNCTION: LEAST SQUARES ΔX	LEAST SQUARES ΔY	MOMENT-LS ΔX	MOMENT-LS ΔY	
1-1	0.220	0.096	0.251	0.024	0.077	0.027	κ=0°
1-2	-.010	-.031	0.016	-.027	0.015	-.027	
2-1	-.059	-.005	-.098	-.021	-.098	-.021	
2-2	0.109	-.126	0.005	0.008	0.005	0.008	κ=0°
2-3	-.006	-.045	-.041	0.062	-.041	0.062	
3-1	-.020	-.057	0.216	-.032	0.212	-.031	
3-2	0.014	0.035	-.006	0.019	-.006	0.019	κ=45°
3-3	-.088	0.042	-.008	-.037	-.008	-.037	
4-1	-.103	0.040	0.011	0.020	0.011	0.020	
4-2	0.262	0.288	0.011	-.006	0.011	-.006	
4-3	0.069	-.004	-.004	0.024	-.004	0.022	κ=5°
4-4	0.378	-.027	0.055	0.019	0.059	0.018	
5-1	-.009	-.026	-.151	0.011	-.151	0.012	
5-2	-.009	0.131	-.025	0.033	-.025	0.033	κ=20°
5-3	0.213	-.003	-.045	0.043	0.003	0.066	
6-1	-.049	-.089	-.047	-.084	-.046	-.084	
6-2	0.021	0.100	0.029	-.028	0.029	-.028	
6-3	-.057	0.031	-.026	-.026	-.051	0.016	κ=45°
6-4	-.053	0.083	-.019	0.020	-.019	0.020	
RMS	0.136	0.093	0.090	0.034	0.071	0.035	
RMS (XY)	0.165		0.096		0.079		

TABLE 7.

IMAGE TARGET	MOMENT ΔX	MOMENT ΔY	GAUSSIAN SPREAD FUNCTION: LEAST SQUARES ΔX	LEAST SQUARES ΔY	MOMENT-LS ΔX	MOMENT-LS ΔY	
1-1	0.220	0.096	0.087	0.059	0.058	0.044	κ=0°
1-2	-.010	-.034	0.016	-.033	0.016	-.031	
2-1	-.059	-.005	-.077	-.029	-.077	-.029	
2-2	0.109	-.126	0.004	0.009	-.003	-.009	κ=0°
2-3	-.006	-.045	-.030	0.052	-.030	0.053	
3-1	-.020	-.057	0.033	-.013	0.034	-.012	
3-2	0.014	0.035	-.022	0.002	-.020	0.001	κ=45°
3-3	-.088	0.042	-.018	-.032	-.019	-.032	
4-1	-.103	0.040	0.005	0.041	0.006	0.041	
4-2	0.262	0.288	0.092	0.040	0.094	0.038	
4-3	0.069	-.004	-.001	0.030	-.001	0.031	κ=5°
4-4	0.378	-.027	0.063	-.025	0.062	-.027	
5-1	-.009	-.026	-.107	0.048	-.109	0.047	
5-2	-.009	0.131	-.024	0.031	-.025	0.030	κ=20°
5-3	0.213	-.003	-.017	0.034	-.010	0.037	
6-1	-.049	-.089	-.029	-.051	-.030	-.051	
6-2	0.021	0.100	0.036	0.009	0.036	0.009	
6-3	-.057	0.031	-.014	0.001	-.014	0.001	κ=45°
6-4	-.053	0.083	-.022	0.040	-.023	0.040	
RMS	0.136	0.093	0.048	0.035	0.046	0.034	
RMS (XY)	0.165		0.059		0.057		

TABLE 8.

NO.	CASE A MOMENT, M Δx	CASE A MOMENT, M Δy	CASE B M/LS (3) Δx	CASE B M/LS (3) Δy	CASE C M/LS (5) Δx	CASE C M/LS (5) Δy	CASE D M/LS (5 + 2) Δx	CASE D M/LS (5 + 2) Δy
1	-0.218	0.072	-0.023	-0.060	-0.023	-0.060	-0.026	-0.054
2	0.030	-0.033	0.038	0.013	-0.038	0.013	0.042	-0.023
3	0.026	0.255	0.021	-0.036	0.020	-0.036	0.013	-0.014
4	-0.243	0.057	0.056	0.006	0.056	0.006	0.053	0.033
5	0.307	-0.222	0.012	0.011	0.012	0.011	0.039	0.007
6	0.370	0.040	0.079	0.038	0.079	0.038	0.101	0.036
7	-0.306	0.100	-0.057	0.041	-0.057	0.041	-0.054	0.034
8	-0.147	-0.109	-0.075	0.037	-0.075	0.036	-0.091	0.003
9	0.097	-0.106	-0.048	-0.005	-0.048	-0.005	-0.047	-0.005
10	-0.047	0.223	-0.023	0.028	-0.021	0.028	-0.026	0.028
11	0.049	0.079	-0.039	-0.047	-0.039	-0.047	-0.060	-0.021
12	-0.127	0.097	-0.025	0.016	-0.025	0.016	0.006	0.033
13	0.171	-0.110	-0.010	0.040	-0.011	0.041	0.004	0.037
14	-0.104	0.351	0.099	-0.224	-0.010	-0.011	-0.082	0.059
15	0.354	0.087	-0.023	-0.026	-0.023	-0.026	-0.012	-0.029
16	0.082	0.018	0.004	0.027	0.003	0.027	-0.008	0.022
17	-0.372	0.215	0.026	-0.034	0.026	-0.034	0.019	-0.018
18	0.066	-0.068	0.034	0.044	0.033	0.044	0.032	0.042
19	-0.333	0.301	-0.053	-0.083	-0.053	-0.083	-0.111	-0.020
20	-0.071	0.407	0.002	0.027	0.002	0.027	-0.019	0.020
21	0.222	0.092	0.141	-0.058	0.142	-0.058	0.099	-0.017
22	-0.091	0.302	-0.098	0.025	-0.098	0.026	-0.058	0.025
23	0.049	0.005	0.012	0.015	0.012	0.015	0.012	0.016
24	0.108	0.125	0.000	0.018	0.002	0.017	0.009	0.018
25	0.122	-0.190	0.035	0.029	0.035	0.029	0.036	0.029
RMS	0.200	0.182	0.059	0.057	0.050	0.036	0.053	0.029